

# Function of BRCA1 in the DNA Damage Response Is Mediated by ADP-Ribosylation

Mo Li<sup>1</sup> and Xiaochun Yu<sup>1,\*</sup>

<sup>1</sup>Division of Molecular Medicine and Genetics, Department of Internal Medicine, University of Michigan Medical School, Ann Arbor, MI 48109, USA

\*Correspondence: [xiayu@umich.edu](mailto:xiayu@umich.edu)

<http://dx.doi.org/10.1016/j.ccr.2013.03.025>

## SUMMARY

Carriers of *BRCA1* germline mutations are predisposed to breast and ovarian cancers. Accumulated evidence shows that *BRCA1* is quickly recruited to DNA lesions and plays an important role in the DNA damage response. However, the mechanism by which *BRCA1* is recruited to DNA damage sites remains elusive. *BRCA1* forms a Ring-domain heterodimer with *BARD1*, a major partner of *BRCA1* that contains tandem *BRCA1* C-terminus (BRCT) motifs. Here, we identify the BRCTs of *BARD1* as a poly(ADP-ribose) (PAR)-binding module. The binding of the *BARD1* BRCTs to PAR targets the *BRCA1/BARD1* heterodimer to DNA damage sites. Thus, our study uncovers a PAR-dependent mechanism of rapid recruitment of *BRCA1/BARD1* to DNA damage sites.

## INTRODUCTION

Cells encounter numerous environmental and internal hazards that induce various kinds of DNA damage. To cope with these threats, cells have developed a DNA damage response system to sense and repair DNA lesions. Loss of this DNA damage response leads to the accumulation of DNA lesions, triggers genomic instability, and ultimately promotes tumorigenesis. Thus, many DNA damage response proteins are important tumor suppressors.

*BRCA1* is a breast and ovarian cancer suppressor (Miki et al., 1994). Germline *BRCA1* mutation carriers are predisposed to breast and ovarian cancers (King et al., 2003; Rahman and Stratton, 1998; Turner et al., 2004; Venkitaraman, 2002). Accumulated evidence suggests that *BRCA1* plays important roles in several biological events during the DNA damage response including cell cycle checkpoint activation and repair of DNA double-strand breaks (DSBs) (Huen et al., 2010; Roy et al., 2011; Scully et al., 1997; Scully and Livingston, 2000). As a result, tumor cells bearing *BRCA1* mutations are hypersensitive to DSB-inducing agents, such as ionizing radiation (IR) (Abbott et al., 1999; Shen et al., 1998). In addition to DSB repair, cells have other pathways to repair different types of DNA

lesions, such as DNA single-strand breaks (SSBs). It has been shown that poly(ADP-ribose) polymerases (PARPs) play important roles in SSB repair (Bürkle, 2001; Fisher et al., 2007; Okano et al., 2003). It is interesting that suppression of PARPs by inhibitors can specifically kill breast cancer cells bearing *BRCA1* mutations. It has been hypothesized that cells lacking both PARP-dependent SSB repair and *BRCA1*-dependent DSB repair are inviable (Farmer et al., 2005; Fong et al., 2009; Rouleau et al., 2010). Following DNA damage, PARP1, one of the major PARPs in the DNA damage response, quickly relocates to DNA damage sites and catalyzes protein PARylation (Kim et al., 2005). Although the function of this PARylation is not clear, some evidence suggests that it can function as a docking signal to recruit other DNA damage response factors to DNA lesions (Masson et al., 1998; Okano et al., 2003; Ruscetti et al., 1998). It is interesting that recent structural analyses indicate that PARP1 also recognizes DSBs (Ali et al., 2012), although the function of PARP1 in DSB repair is unknown.

Like PARP1, *BRCA1* is also quickly recruited to DNA damage sites (Scully et al., 1997). The molecular mechanism by which *BRCA1* is recruited to DNA damage sites remains elusive. Two important DNA damage response factors,  $\gamma$ H2AX and MDC1, have been shown to facilitate the recruitment of *BRCA1* to

## Significance

Familial breast cancers are often derived from germline mutations of *BRCA1*, with mutation carriers having an ~90% lifetime risk of developing breast cancer. Poly(ADP-ribose) polymerase (PARP) inhibitors selectively kill *BRCA1*-deficient cells, and several PARP inhibitors are currently in breast cancer clinical trials. However, the mechanism underlying the sensitivity of tumor cells bearing *BRCA1* mutations to PARP inhibition is not clear. Here, we found that PARP inhibition directly suppresses the fast recruitment of the *BRCA1/BARD1* heterodimer to DNA damage sites and impairs DNA repair. These findings suggest a mechanism by which PARP inhibitors specifically kill breast cancer cells bearing *BRCA1* mutations.

DNA damage sites (Harper and Elledge, 2007). However, BRCA1 can still be transiently recruited to DNA damage sites in the absence of  $\gamma$ H2AX, although it cannot be stably retained at DNA damage sites (Celeste et al., 2003), suggesting that H2AX provides the platform to stabilize BRCA1 at DNA damage sites instead of directly recruiting it. Recently, it has been shown that a DNA damage-induced protein ubiquitination pathway governs the relocation of BRCA1 to sites of DNA damage via the RAP80 complex (Kim et al., 2007; Sobhian et al., 2007; Wang et al., 2007). However, deletion of RAP80 does not completely abolish the IR-induced foci formation of BRCA1 (Hu et al., 2011), suggesting that alternative mechanism of recruitment of BRCA1 to DNA damage sites exists. Since the DNA damage-induced protein ubiquitination pathway is  $\gamma$ H2AX-dependent (Huen et al., 2007; Kolas et al., 2007; Mailand et al., 2007), it is likely that protein ubiquitination at DNA damage sites, like  $\gamma$ H2AX, only stabilizes BRCA1 foci instead of acting in the initial recruitment of BRCA1. Thus, in this study, we examined the molecular mechanism by which BRCA1 is recruited to the sites of DNA damage.

## RESULTS

### BARD1 Mediates the Rapid Recruitment of BRCA1 to DNA Damage Sites

To search for the molecular mechanism by which BRCA1 is recruited to DNA damage sites, we measured the kinetics of BRCA1's relocation to sites of DNA damage. Using laser microirradiation and live cell imaging, we found that BRCA1 was rapidly recruited to sites of DNA damage within 20 s following laser microirradiation in mouse embryonic fibroblasts (MEFs) (Figure 1A). In  $H2AX^{-/-}$  MEFs, BRCA1 was still recruited to DNA damage sites within 20 s. However, the majority of the BRCA1 dissociated from the DNA damage sites within 5 min following laser microirradiation (Figure 1A). Thus, these results are in agreement with a previous report that H2AX is important for BRCA1 retention but not for its initial recruitment to DNA damage sites (Celeste et al., 2003).

BRCA1 contains an N-terminal Ring domain and tandem BRCA1 C-terminal motifs (BRCTs), forming a BRCT domain. We next examined the importance of these two domains to the recruitment of BRCA1. It is well known that the tandem BRCA1 BRCT motifs recognize phosphoserine (pSer) motifs and are involved in targeting BRCA1 to DNA damage sites (Manke et al., 2003; Yu et al., 2003). Either S1655A or K1702A mutation in the BRCA1 BRCTs abolishes pSer binding (Botuyan et al., 2004; Clapperton et al., 2004; Williams et al., 2004). Unexpectedly, both mutated forms of BRCA1 were still recruited to DNA damage sites within 20 s after laser microirradiation. However, neither could be stably accumulated at DNA damage sites, and both dissociated from the DNA damage sites within 5 min (Figure 1B). These results suggest that the BRCT domain of BRCA1 is required for the retention of BRCA1 at DNA damage sites but not for the initial, rapid recruitment of BRCA1 to sites of DNA damage. To confirm our conclusion, we expressed the recombinant BRCT domain of BRCA1 in wild-type (WT) MEFs. The BRCA1 BRCTs slowly accumulated at DNA damage sites and could be visualized there within ~10 min following laser microirradiation (Figure 1C). Moreover, the BRCA1 BRCTs failed

to be recruited to DNA damage sites in the absence of H2AX (Figure 1C), suggesting that H2AX is required for the BRCT-dependent BRCA1 retention at DNA damage sites.

Since the BRCA1 BRCT motifs do not directly target BRCA1 to DNA damage sites during the early DNA damage response, we searched for other possible factors that might facilitate the relocation of BRCA1. Beside the C-terminal BRCTs, BRCA1 contains an N-terminal Ring domain (Koonin et al., 1996). It has been reported that the Ring domain of BRCA1 is important for IR-induced BRCA1 foci formation (Au and Henderson, 2005). To explore the role of the Ring domain in the recruitment of BRCA1 to sites of DNA damage, we generated the C61G mutation in BRCA1 that abolishes the structure of the Ring domain. It is interesting that BRCA1 bearing the C61G mutation failed to be rapidly recruited to DNA damage sites following laser microirradiation treatment but retained its ability to accumulate at later times (Figure 1D). These observations suggest that the Ring domain of BRCA1 is required for its early recruitment to DNA damage sites. Moreover, the slow accumulation of the C61G mutant was abolished in  $H2AX^{-/-}$  MEFs (Figure 1D), further suggesting that the H2AX-dependent pathway maintains the stability of BRCA1 at DNA damage sites.

The Ring domain of BRCA1 associates with the Ring domain of BARD1, which forms a Ring domain heterodimer and functions as an E3 ubiquitin ligase (Hashizume et al., 2001; Meza et al., 1999; Wu et al., 1996). However, this Ring domain heterodimer per se could not relocate to DNA damage sites (Au and Henderson, 2005), suggesting that BARD1, the Ring domain partner of BRCA1, may target the heterodimer to DNA damage sites. Like BRCA1, BARD1 quickly relocates to DNA damage sites regardless of the status of H2AX, and H2AX is also required for the retention of BARD1 at DNA damage sites (Figure 1E).

Similar to BRCA1, BARD1 has tandem BRCT motifs at its C terminus. However, unlike the BRCA1 BRCTs, the isolated BARD1 BRCTs relocated to DNA damage sites within 20 s after laser microirradiation but dissociated within 5 min. Moreover, the relocation of the BARD1 BRCTs to DNA damage sites was independent of the status of H2AX (Figure 1F). To rule out the possibility that the relocation kinetics fluctuated based on transfection efficiency in each experiment, we transfected the  $H2AX^{-/-}$  MEFs with a high concentration (0.6  $\mu$ g/1.5 cm glass-bottomed dish) and a low concentration (0.2  $\mu$ g/1.5 cm glass-bottomed dish) of plasmids encoding green fluorescent protein (GFP)-BARD1 BRCT domain and then investigated the relocation kinetics of BARD1 BRCT domain following laser microirradiation. As shown in Figure S1A available online, different protein expression levels did not affect the relocation kinetics. These results suggest that the BARD1 BRCTs might target BRCA1 to DNA damage sites during the early DNA damage response. Structural analysis of the BARD1 BRCTs suggests that, similar to the pSer-binding pocket of the BRCA1 BRCTs, the tandem BARD1 BRCTs fold together and form a binding pocket with K619 as a key residue (Birrane et al., 2007). Thus, we generated a K619A mutant of the BARD1 BRCTs. This mutant form failed to relocate to DNA damage sites, suggesting that this potential binding pocket is important for the rapid relocation of BARD1 to DNA damage sites (Figure 1F).

Next, we asked whether K619 of BARD1 is also important for the recruitment of BRCA1 to DNA damage sites. U2OS cells

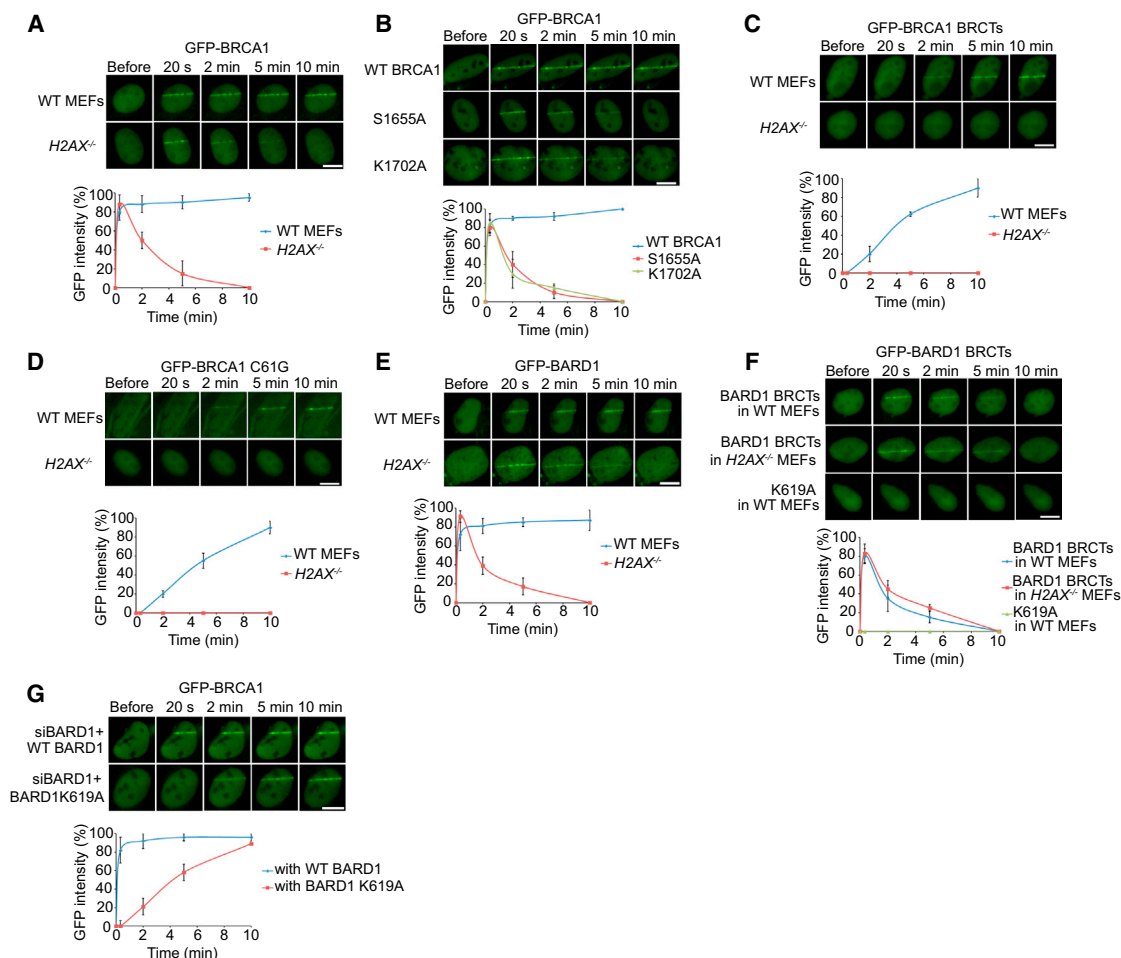


**Figure 1. The Recruitments of BRCA1 and BARD1 to DNA Damage Sites**

(A) The relocation kinetics of BRCA1 to DNA damage sites. GFP-BRCA1 was expressed in WT or H2AX<sup>-/-</sup> MEFs. The relocation kinetics was monitored in a time course following laser microirradiation (the same for below).  
(B) The relocation kinetics of the S1655A or K1702A mutants of BRCA1 to DNA damage sites. GFP-WT BRCA1, S1655A, or K1702A mutants were expressed in U2OS cells.  
(C) The relocation kinetics of the BRCA1 BRCTs to DNA damage sites. The GFP-BRCA1 BRCT domain was expressed in WT or H2AX<sup>-/-</sup> MEFs.  
(D) The relocation kinetics of the C61G mutant of BRCA1 to DNA damage sites. The GFP-BRCA1 C61G mutant was expressed in WT or H2AX<sup>-/-</sup> MEFs.  
(E) The relocation kinetics of BARD1 to DNA damage sites. GFP-BARD1 was expressed in WT or H2AX<sup>-/-</sup> MEFs.  
(F) The relocation kinetics of the BARD1 BRCTs and the K619A mutant to DNA damage sites. GFP-WT BARD1 BRCT domain or the K619A mutant was expressed in WT or H2AX<sup>-/-</sup> MEFs.  
(G) The effect of the BARD1 K619A mutant on the recruitment of BRCA1 to DNA damage sites. U2OS cells stably expressing siRNA-resistant WT BARD1 or the K619A mutant were transfected with BARD1 siRNA to deplete endogenous BARD1. GFP-BRCA1 was expressed in these stable cell lines. GFP fluorescence at the laser line was converted into a numerical value (relative fluorescence intensity) using Axiovision software (version 4.5). Normalized fluorescent curves from 20 cells from three independent experiments were averaged. The error bars represent the SD. Scale bar, 10  $\mu$ m.  
See also Figure S1.

stably expressing either small interfering RNA (siRNA)-resistant WT BARD1 or siRNA-resistant K619A mutant were treated with BARD1 siRNA to deplete endogenous BARD1 (Figures S1B and S1C). When cells were treated with laser microirradiation, BRCA1 quickly relocated to DNA damage sites in the presence of WT BARD1 but not the K619A mutant, suggesting that the BARD1 BRCTs are critical for targeting BRCA1 to DNA lesions during early DNA damage response (Figure 1G). However, the BARD1 BRCTs mutation did not impair the slow accumulation of BRCA1 to DNA damage sites (Figure 1G). We also generated the L44P mutation in the BARD1 Ring domain, which abolishes

BRCA1/BARD1 heterodimer formation (Morris et al., 2002). Like the C61G mutation in the BRCA1 Ring domain, the BARD1 L44P mutant could not facilitate the early recruitment of BRCA1 to DNA damage site (Figure S1D). Taken together, these results suggest that the early recruitment of BRCA1 to DNA damage sites is mediated by the BARD1 BRCTs.

#### The BARD1 BRCTs Bind PAR In Vitro and In Vivo

Next, we sought the binding partner of the BARD1 BRCTs. Since the relocation kinetics of the BARD1 BRCTs to DNA damage sites is very similar to that of PAR at DNA damage sites (Gibson

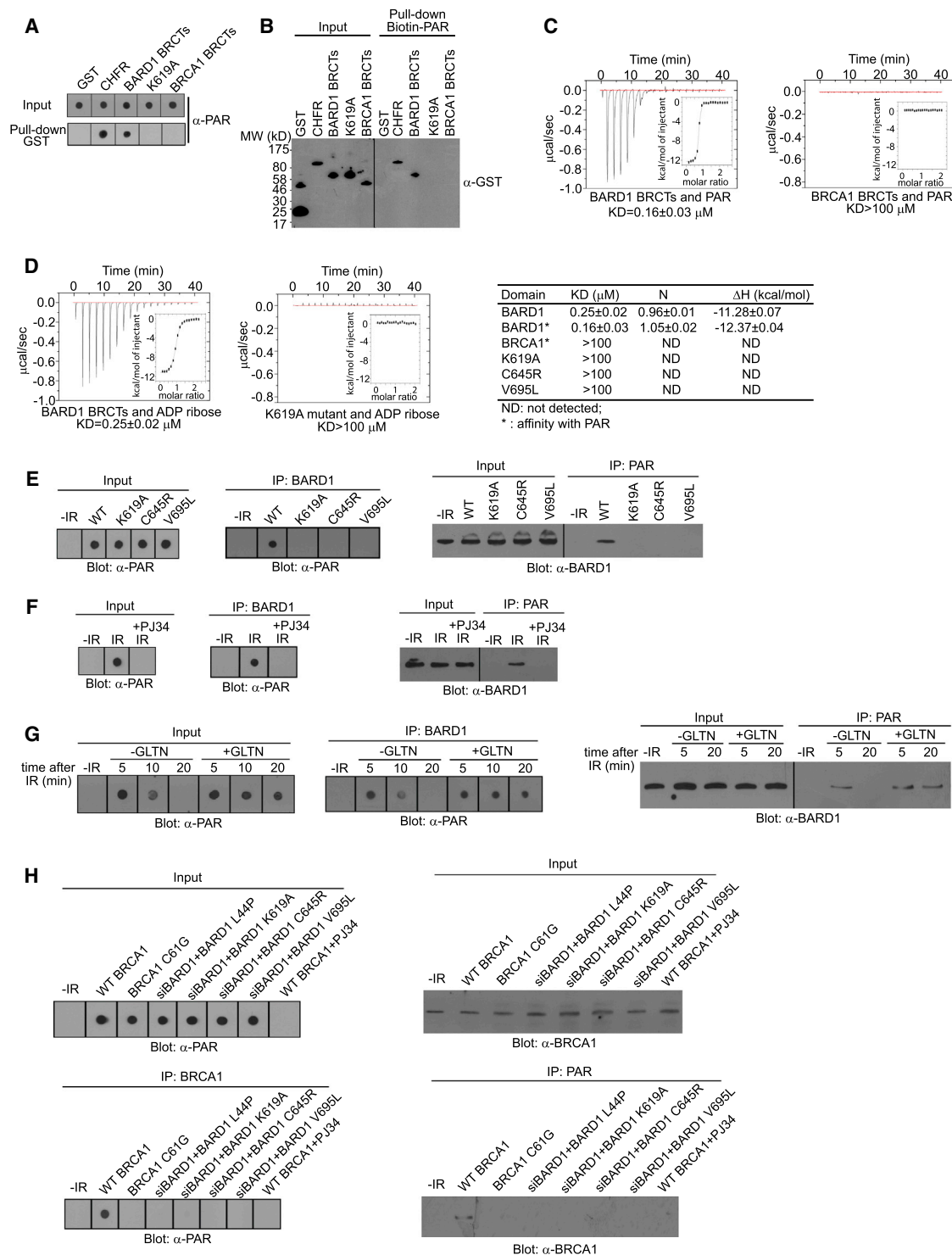


**Figure 2. The BARD1 BRCTs Directly Bind PAR**

(A) The interaction between GST (negative control), GST-CHFR (positive control), GST-BARD1 BRCTs, GST-BARD1 BRCTs K619A mutant, or GST-BRCA1 BRCTs and PAR was examined by dot blot using anti-PAR antibody. PAR was blotted and shown as the input.

(B) The interaction between the recombinant proteins in (A) and biotin-PAR was examined by the reciprocal pull-down assay with anti-GST antibody. Recombinant proteins were blotted and shown as the input.

(C) The affinity between GST-BARD1 BRCTs or GST-BRCA1 BRCTs and PAR was measured by ITC. Titration of PAR was injected into a solution containing the purified protein. The inset shows the fit of the data to an equilibrium-binding isotherm. The fit provides an equilibrium dissociation constant ( $K_D$ ) for the binding of PAR to the protein.

(legend continued on next page)



and Kraus, 2012; Kim et al., 2005), we hypothesized that the BARD1 BRCTs may recognize PAR. We synthesized and purified PAR from an established *in vitro* assay (Fahrer et al., 2007; Kiehlbauch et al., 1993) and generated recombinant BARD1 BRCTs and the K619A mutant. The WT BARD1 BRCTs, but not the K619A mutant, could directly coimmunoprecipitate PAR (Figure 2A). Moreover, a reciprocal pull-down further confirmed the direct interaction between the BARD1 BRCTs and PAR (Figure 2B). Next, we measured the affinity between the BARD1 BRCTs and PAR using Isothermal Titration Calorimetry (ITC) (Figure 2C). The dissociation constant,  $K_D$ , was  $\sim 0.16 \mu\text{M}$ , which is very similar to the affinity between the BRCA1 BRCTs and pSer peptide and the affinity between PAR and its other binding partners (Karras et al., 2005; Yu et al., 2003). Of note, unlike the BARD1 BRCTs, the BRCA1 BRCTs did not interact with PAR (Figures 2A–2C).

Since PAR is a branched polymer of ADP-ribose, we could not precisely determine the structure of PAR synthesized both *in vitro* and *in vivo*. Thus, the affinity between the BARD1 BRCTs and PAR might not have been measured accurately by ITC. To clarify this, we measured the affinity between the BARD1 BRCTs and ADP-ribose, the basic unit of PAR. This  $K_D$  was  $\sim 0.25 \mu\text{M}$ , which is again similar to the affinity between other PAR-binding domains and ADP-ribose (Karras et al., 2005). To further examine the interaction between the BARD1 BRCTs and PAR, we performed a competition experiment using excess ADP-ribose in the pull-down and reciprocal pull-down assays. In these assays, we used 30- to 50-mer PAR. At a 100:1 M ratio between free ADP-ribose and PAR, ADP-ribose could significantly suppress the interaction between the BARD1 BRCTs and PAR (Figure S2A). The results support our interpretation that the BARD1 BRCTs bind each ADP-ribose in PAR. Moreover, we could not detect any interaction between the K619A mutant and ADP-ribose, suggesting that K619A mutation abolishes the BARD1 ADP-ribose binding pocket (Figure 2D).

A previous study suggests that the BARD1 BRCT may selectively recognize the pSDDE motif (Rodriguez et al., 2003). However, the affinity between the XXXXpSDDE peptide (“X” stands for random amino acid) and the BARD1 BRCTs was much weaker than that between PAR and the BARD1 BRCTs (Figure S2B). Accordingly, the pSer peptide could not compete away the interaction between PAR and the BARD1 BRCTs in the same manner as ADP-ribose (Figure S2C).

Germline mutations in the BARD1 BRCTs have been identified in familial breast cancer patients (Ishitobi et al., 2003; Sauer and Andrusis, 2005; Thai et al., 1998). We randomly picked two of these mutations, C645R and V695L, for further study. The BARD1 BRCTs bearing either mutation failed to bind PAR (Figure 2D; Figure S2D).

Next, we asked whether BARD1 could interact with PAR *in vivo*. Proteins with long PAR chains (>100 ADP-ribose) cannot

easily migrate into the SDS-PAGE because of the size and phosphate moieties in PAR (Figure S2E). Thus, we used dot blot to examine PAR binding *in vivo*, which is a better approach to recover the long PAR chains during the analysis (Affar et al., 1998; Fiorillo et al., 2005; Vilchez Larrea et al., 2011). Following DNA damage, PAR is quickly synthesized at the DNA damage sites (D’Amours et al., 1999; Kim et al., 2005). Thus, without DNA damage, we could not detect PAR *in vivo* (Figure 2E). Following IR treatment, not only could we detect PAR, but we also found that PAR interacted with BARD1 using coimmunoprecipitation (co-IP) assays. The results were further confirmed by reciprocal co-IP (Figure 2E). Moreover, BARD1 itself was not PARylated (Figure S2F), and the K619A, C645R, and V695L mutants of BARD1 could not interact with PAR (Figure 2E), which is consistent with the *in vitro* analysis. Next, we treated cells with PJ34, a potent PARP inhibitor, to suppress PAR synthesis at DNA damage sites. With PJ34 treatment, BARD1 could no longer interact with PAR after IR treatment (Figure 2F).

Immediately following DNA damage, the PAR that is synthesized in a few seconds by PARPs is hydrolyzed quickly by PAR glycohydrolase (PARG) (D’Amours et al., 1999; Kim et al., 2005). Without any treatment, the BARD1/PAR complex is diminished within 20 min following IR. However, when we pretreated cells with gallotannin (GLTN), a cell-permeable PARG inhibitor that suppresses PAR degradation *in vivo* (Fathers et al., 2012; Ying et al., 2001), DNA damage-induced PAR remained elevated. Thus, we could detect the BARD1/PAR complex in a significantly prolonged period following DNA damage (Figure 2G).

Since BRCA1 forms a stable complex with BARD1, we asked whether BRCA1 also associates with PAR *in vivo*. As shown in Figure 2H, WT BRCA1 did associate with PAR *in vivo* following IR treatment. However, the C61G mutation that disrupts the interaction with BARD1 also abolished the PAR interaction. Moreover, cells depleted of endogenous BARD1 by siRNA and reconstituted with the L44P, K619A, C645R, or V659L BARD1 mutants lacked the interaction between BRCA1 and PAR (Figure 2H). Taken together, these results demonstrate that the BARD1 BRCTs interact with PAR both *in vitro* and *in vivo* and mediate an association of BRCA1 with PAR *in vivo*.

### PARP Inhibition Suppresses the Early Recruitment of the BRCA1/BARD1 Complex to DNA Lesions

Accumulated evidence shows that cells bearing BRCA mutations are hypersensitive to PARP inhibitors (Bryant et al., 2005; Farmer et al., 2005; Rouleau et al., 2010). Since the BARD1 BRCTs bind PAR, we examined the effects of PARP inhibitor treatment on the recruitment of BRCA1 to DNA damage sites. As expected, PAR was quickly synthesized at DNA damage sites, appearing within less than 1 min, and almost degraded

(D) The affinity between GST-BARD1 BRCTs or GST-BARD1 BRCTs K619A mutant and ADP-ribose was measured by ITC (left and middle, respectively). Affinities between the BRCA1 BRCTs, BARD1 BRCTs, or BARD1 BRCTs mutants and ADP ribose or PAR are summarized in the table (right).

(E) The *in vivo* interaction between BARD1 or the mutants and PAR was measured by co-IP and reciprocal co-IP.

(F) The *in vivo* interaction between BARD1 and PAR with or without the treatment of PJ34 was measured by co-IP and reciprocal co-IP.

(G) The *in vivo* interaction between BARD1 and PAR with or without the treatment of GLTN was measured by co-IP and reciprocal co-IP.

(H) The *in vivo* interaction between WT BRCA1, BRCA1 C61G, or WT BRCA1 with the indicated BARD1 mutants and PAR was measured by co-IP and reciprocal co-IP. Whole cell lysates were blotted and shown as the input in (E) through (H).

See also Figure S2.

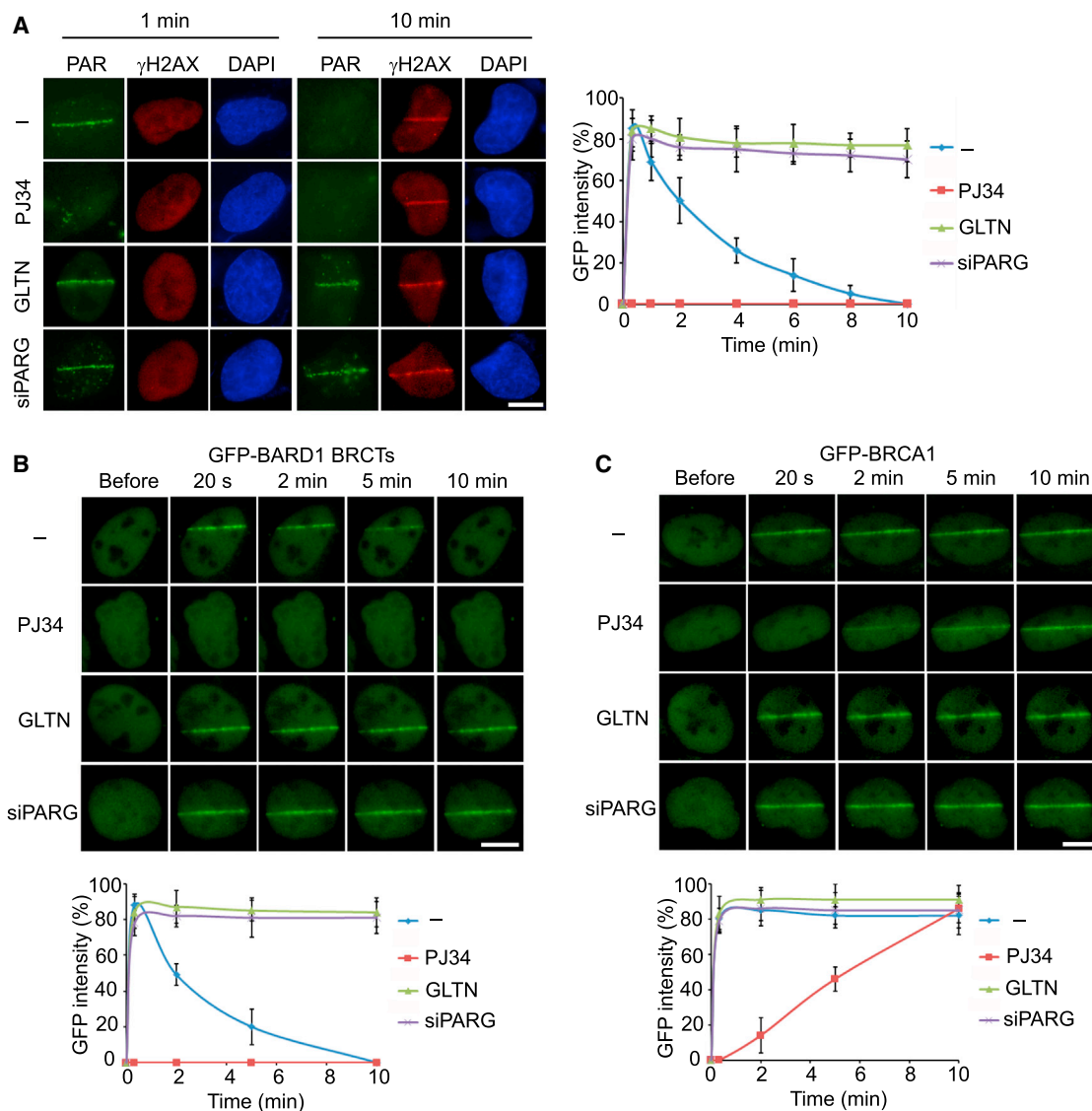


**Figure 3. The Effect of PARP Inhibitor on the Recruitment of the BRCA1/BARD1 Heterodimer to DNA Lesions during Early DNA Damage Response**

(A) Representative staining of PAR and  $\gamma$ H2AX in cells pretreated by PJ34, GLTN, or PARG knockdown at 1 min or 10 min after laser microirradiation (left). Cells pretreated by PJ34, GLTN, or PARG knockdown were fixed at the indicated time points after laser microirradiation, and the kinetics of PAR staining was examined and summarized in the panel graph (right).

(B) The effects of PJ34, GLTN, and PARG knockdown on the recruitment of BARD1 BRCTs to DNA damage sites. GFP-BARD1 BRCT domain was expressed in U2OS cells pretreated by PJ34, GLTN, or PARG knockdown. The relocation of GFP-BARD1 BRCTs was monitored in a time course following laser microirradiation.

(C) The effects of PJ34, GLTN, and PARG knockdown on the recruitment of BRCA1 to DNA damage sites. GFP-BRCA1 was expressed in U2OS cells pretreated by PJ34, GLTN, or PARG knockdown. The relocation of BRCA1 to DNA damage sites was monitored in a time course following laser microirradiation. GFP fluorescence at the laser line was converted into a numerical value (relative fluorescence intensity) using Axiovision software (version 4.5). Normalized fluorescent curves from 20 cells from three independent experiments were averaged. Error bars represent the SD. Scale bar, 10  $\mu$ m.

See also Figure S3.

within 10 min following laser microirradiation (Figure 3A). With PJ34 treatment to suppress PARP activity, we could not detect PAR at DNA damage sites (Figure 3A; Figure S3A). However, PJ34 treatment did not affect the phosphorylation of H2AX at DNA damage sites (Figure 3A; Figure S3B), suggesting that laser microirradiation still induced DNA damage when cells were treated with PJ34. With GLTN treatment or PARG knockdown

(Figure S1B) to suppress PARG activity, PAR could be detected at DNA damage sites for a prolonged period (Figure 3A).

We next examined the relocation kinetics of the BARD1 BRCTs to DNA damage sites. Similar to the kinetics of PAR at DNA damage sites, PJ34 treatment abolished the recruitment of the BARD1 BRCTs to DNA damage sites (Figure 3B; Figure S3A), whereas GLTN treatment or PARG knockdown

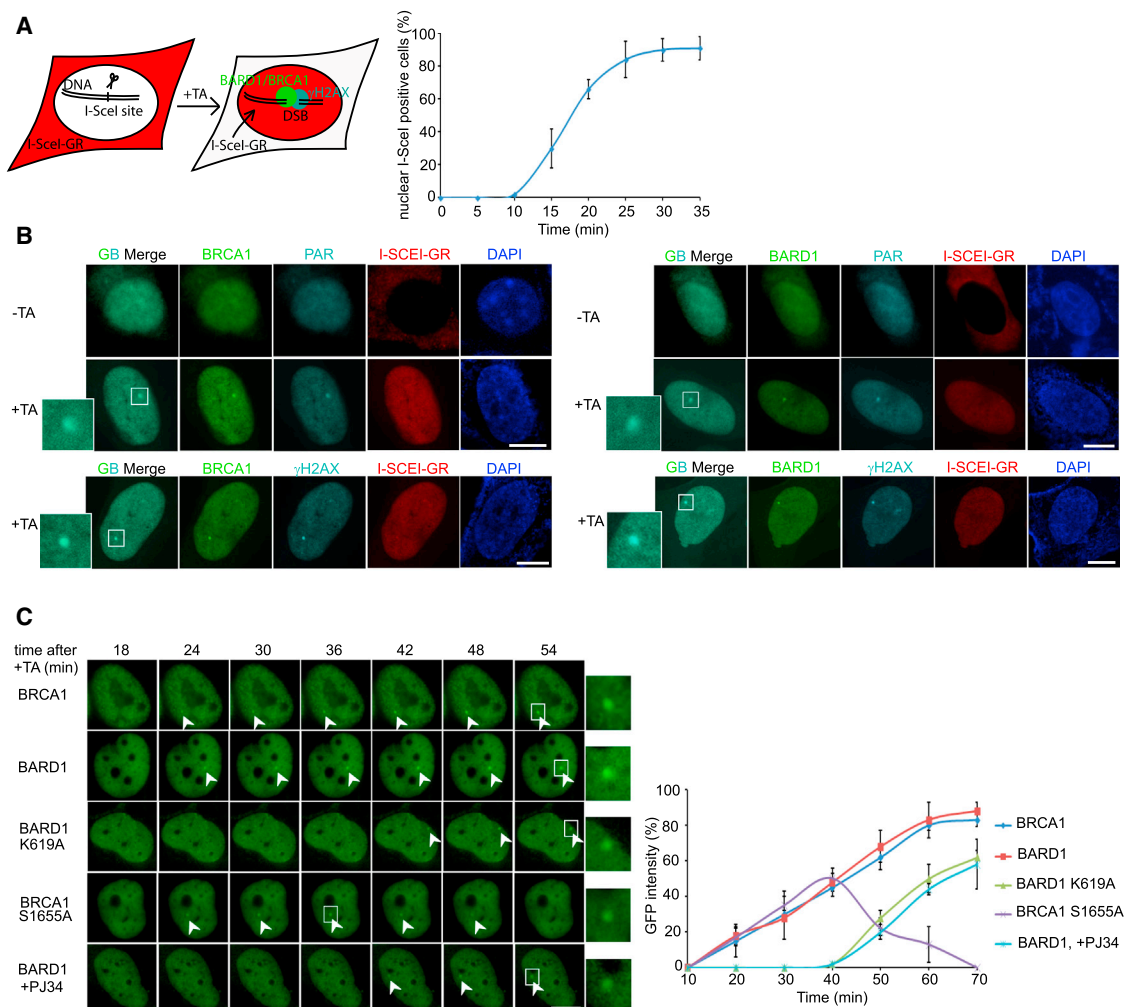


**Figure 4. The Recruitment of BRCA1/BARD1 Complex to DSB**

(A) Schematics of the inducible I-SceI system. TA treatment induces the translocation of RFP-I-SceI-GR fusion protein (red) from the cytoplasm to the nucleus (left). A time course shows the translocation kinetics of RFP-I-SceI-GR from the cytoplasm to the nucleus after TA addition (right).

(B) The localization of BRCA1 or BARD1 and PAR before and after TA induction. The DSB (focus) was also marked by  $\gamma$ H2AX. Magnified boxes denote the colocalization of BRCA1 or BARD1 with PAR or  $\gamma$ H2AX at the DSB.

(C) Real-time images of the recruitments of GFP-BRCA1, GFP-BARD1, and their GFP mutants in the inducible I-SceI system. Magnified boxes denote the GFP fusion proteins at focus. Error bars represent the SD. Scale bar, 10  $\mu$ m.

significantly prolonged the retention (Figure 3B). A similar relocation kinetics of BRCA1 to DNA damage sites was also observed with these treatments (Figure 3C). The fast relocation of the BARD1 BRCTs and BRCA1 to DNA damage sites was also suppressed by the distinct PARP inhibitors olaparib and ABT-888 (Figures S3C and S3D). We further confirmed the results using *Parp1*<sup>-/-</sup> MEFs (Figure S3E), in which the early recruitment of BARD1, the BARD1 BRCTs, and BRCA1 were all impaired. Although a small amount of BARD1 and BARD1 BRCTs was still recruited to DNA lesions during the early DNA damage response in *Parp1*<sup>-/-</sup> MEFs, it is likely due to the small amount PAR synthesized at DNA lesions in the *Parp1*<sup>-/-</sup> cells, since PARP1 synthesizes most but not all of the PAR in response to DNA damage (Kim et al., 2005; Schreiber et al., 2006). Collectively, these data suggest that BRCA1 is recruited by PAR during the early DNA damage response.

### BRCA1/BARD1 Is Quickly Recruited to an I-SceI-Induced DSB

Laser microirradiation not only induces DSBs but might also generate SSBs. Since BRCA1 mainly participates in HR repair for DSBs, we wondered whether PAR mediates the recruitment of BRCA1 to DSBs. We adopted an inducible I-SceI system to generate a single DSB in vivo (Soutoglou et al., 2007). I-SceI was fused with glucocorticoid receptor (GR) and red fluorescent protein (RFP). Through triamcinolone acetonide (TA) induction, I-SceI translocated into the nucleus between 10 to 20 min, and its location was monitored by RFP fluorescence (Figure 4A). Twenty minutes following TA induction, we observed a single BRCA1 and BARD1 focus, which colocalized with a PAR focus (Figure 4B). The focus of BRCA1 or BARD1 also colocalized with  $\gamma$ H2AX, the surrogate marker of DSB presence. These results suggest that PAR participates in the DSB-induced DNA damage response.

Using the I-SceI system, we found that both BRCA1 and BARD1 relocated to a DSB very quickly. However, the K619A mutant of BARD1 that disrupts the interaction with PAR could not relocate to the DSB during early DNA damage response. The S1655A mutant of BRCA1 that associates with BARD1 but disrupts the interaction with its phosphoprotein binding partners was recruited to, but not stabilized at, the DSB. Moreover, PJ34 pretreatment abolished the rapid recruitment of BARD1 (Figure 4C). These results are consistent with the relocation kinetics seen with laser microirradiation. It further confirms that the interaction between PAR and BARD1 mediates the early recruitment of the BRCA1/BARD1 complex to DNA damage sites and that the intact BRCA1 BRCTs are critical for the retention (or the slow accumulation) of the BRCA1/BARD1 complex at DNA damage sites.

#### Efficacies of PARP Inhibition on Cancer-Associated BRCA1 and BARD1 Mutants

Since PAR targets the BRCA1/BARD1 complex to DNA damage sites, we examined the effects of PARP inhibition on the recruitments of cancer-associated BRCA1 and BARD1 mutants to DNA damage sites. We first selected several cancer-associated BRCA1 and BARD1 mutants and categorized them into three groups: the BRCA1 BRCT mutants (P1749R and M1775R), the BRCA1 Ring domain mutant (C61G), and the BARD1 BRCT mutants (C645R and V695L). As shown in Figures 5A and 5B, without PJ34 treatment, only the BRCA1 BRCT mutants could rapidly relocate to DNA damage sites. Both the BRCA1 Ring domain mutant and the BARD1 BRCT mutants failed to quickly relocate to DNA damage sites. The BRCA1 Ring domain mutant abolishes the interaction with BARD1; thus, this mutant could only slowly accumulate at DNA damage sites through the intact BRCA1 BRCTs. The BARD1 BRCT mutants abolished the interaction with PAR. Thus, these BARD1 BRCT mutants could only slowly accumulate at DNA damage sites since they associate with WT BRCA1 and the interaction between the BRCA1 BRCTs and pSer motifs is intact. Although the BRCA1 BRCT mutants could quickly relocate to DNA damage sites, they could not stably exist there since these mutations abolish the interaction with the pSer motifs. With PJ34 treatment, which suppresses PAR synthesis at DNA damage sites, the relocation of the BRCA1 BRCT mutants to DNA damage sites was abolished. However, PJ34 treatment affected neither the slow accumulation of the BRCA1 Ring domain mutant nor the BARD1 BRCT mutants.

We then explored the sensitivities of cells with the different BRCA1 and BARD1 mutations to PJ34 during DNA damage. The siRNA-resistant complementary DNA of these mutants was generated. U2OS cells stably expressing these constructs were transfected with siRNA to deplete endogenous BRCA1 or BARD1 (Figures S1B and S1C). Cells were treated with or without PJ34 followed by a low dose of IR. We found that the recruitment to DNA damage sites correlated well with the sensitivity of these cancer-associated BRCA1 and BARD1 mutants to PARP inhibition. Since PARP inhibitor treatment only suppresses the quick recruitment of the BRCA1 BRCT mutants to DNA damage sites, but not the slow accumulation of the BRCA1 Ring domain mutant and the BARD1 BRCT mutants at DNA damage sites, only cells expressing the BRCA1 BRCT mutants

were hypersensitive to PARP inhibitor treatment and IR (Figure 5C). Moreover, we treated cells bearing the P1749R mutation with different doses of PJ34. Only a higher dose of PJ34 that suppressed the relocation of BRCA1 to DNA damage sites could sensitize the cells to IR treatment (Figure 5D). Taken together, these results suggest that PARP inhibition sensitizes cells with BRCA1 BRCT mutant to IR treatment.

#### DISCUSSION

In this study, we identified the BARD1 BRCTs as a PAR-binding motif. DNA damage induces massive PAR synthesis in a very short period of time at DNA lesions (D'Amours et al., 1999; Kim et al., 2005). Previous results suggest that protein PARylation is involved in SSB repair. However, recent structural analysis of PARP1, one of the major PAR polymerases in the DNA damage response, shows that it can recognize DSBs (Ali et al., 2012; Langelier et al., 2012). Our results show that DSBs also induce protein PARylation. Protein PARylation functions as a signal to recruit DNA damage repair proteins like the BRCA1/BARD1 complex to repair DSBs. Suppression of protein PARylation in turn impairs BRCA1/BARD1 recruitment. Our findings also explain the molecular mechanism by which BRCA1/BARD1 is rapidly recruited to DNA damage sites even in the H2AX-deficient cells. Following DSB formation, the BARD1 BRCTs first recognize PAR at DNA lesions, which mediates the rapid recruitment of BRCA1. The retention of BRCA1 is mediated by the BRCA1 BRCTs and is H2AX dependent (Figure S3F). Since SSBs also induce PAR synthesis, it is likely that the BRCA1/BARD1 complex is recruited to SSBs. However, without DNA damage-induced H2AX phosphorylation, the BRCA1/BARD1 complex would be quickly released from DNA damage sites following rapid PAR degradation. Thus, H2AX phosphorylation is still a key factor in facilitating BRCA1 function in DNA damage response.

In our study, the BARD1 BRCTs bind ADP-ribose, the basic unit of PAR, but not phosphoproteins. Although previous peptide library screening showed that the BARD1 BRCT domain preferentially recognizes the pSDDE motif (Rodriguez et al., 2003), the protein-binding partner of the BARD1 BRCTs has not yet been identified. Of note, there are two phosphate groups in one ADP-ribose. The phosphate group of Ser and negatively charged residues following pSer in the pSDDE motif might mimic the negatively charged phosphate groups in ADP-ribose, potentially explaining why pSDDE was identified in library screening. Future structural analysis of the BARD1 BRCTs/ADP-ribose complex should reveal the molecular details of the interaction.

Since the BARD1 BRCTs bind ADP-ribose, free ADP-ribose competed with the BARD1-PAR interaction in vitro. Such competition could not occur in vivo because a high level of free ADP-ribose in vivo is toxic to cells (Dunn et al., 1999; Hassa et al., 2006). The intracellular concentration of ADP-ribose in mammals is maintained below 100  $\mu$ M (Gasser and Guse, 2005) and is tightly controlled by specific ADP-ribose hydrolases/pyrophosphatases, which act as protective factors that limit free ADP-ribose accumulation and protein glycation (D'Amours et al., 1999; Fernández et al., 1996; Hassa et al., 2006; Miró et al., 1989; Ribeiro et al., 1995, 2001). The concentration of NAD<sup>+</sup> in undamaged mammalian cells is around



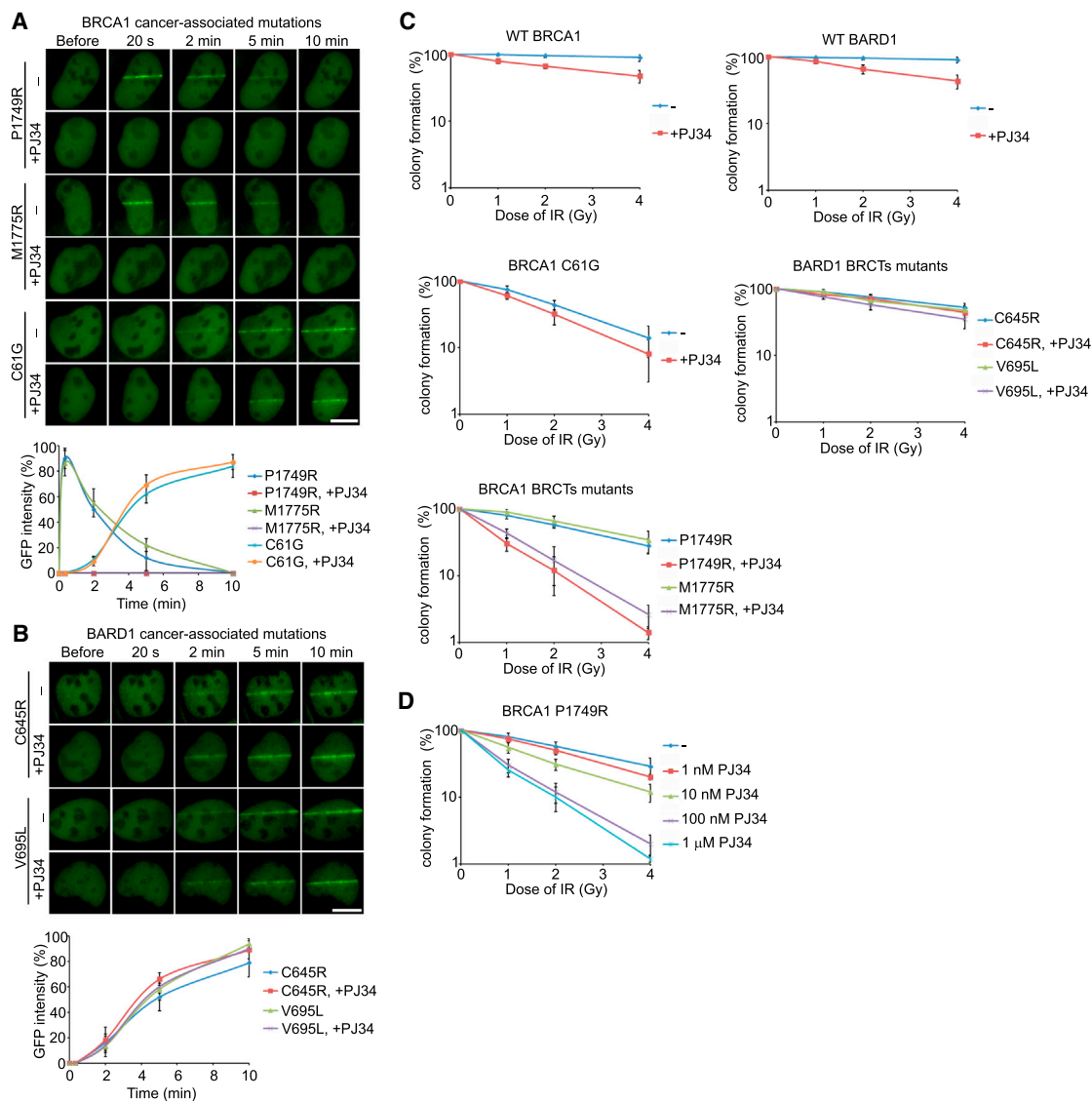


**Figure 5. Efficacy of PARP Inhibitor on Cancer-Associated BRCA1 and BARD1 Mutants**

(A) The effect of PJ34 on the recruitment of the P1749R and M1775R mutants of BRCA1 to DNA damage sites. GFP-BRCA1 mutants were expressed in U2OS cells with or without the treatment of PJ34. The relocation of BRCA1 mutants to DNA damage sites was monitored in a time course following laser microirradiation.

(B) The effect of PJ34 on the recruitment of the C645R and V695L mutants of BARD1 to DNA damage sites. GFP-BARD1 mutants were expressed in U2OS cells with or without the treatment of PJ34. The relocation of BARD1 mutants to DNA damage sites was monitored in a time course following laser microirradiation. Scale bar, 10  $\mu$ m.

(C) The sensitivities of cells bearing cancer-associated BRCA1 or BARD1 mutants to a low dose of IR in the presence or absence of PJ34.

(D) The effect of different doses of PJ34 on the cells bearing the P1749R mutant treated by IR. Error bars represent the SD.

400–500  $\mu$ M, with 65%–75% of  $\text{NAD}^+$  utilized to synthesize PAR in response to DNA damage (D'Amours et al., 1999; Hassa et al., 2006). Thus, free ADP-ribose cannot reach a sufficient concentration to compete away PAR in vivo.

The recruitment of the BRCA1/BARD1 complex to DNA damage sites by PAR is important for cells during the DNA damage response. This process ensures that cells that lose certain phosphorylation-dependent pathways could still repair DNA lesions. It might increase cell viability when cells bear germline or somatic mutations of *BRCA1*. In particular, the most

frequent cancer-associated *BRCA1* mutations are hypomorphic mutations that lose the C-terminal BRCT domain, which is required to bind to functional partners with pSer motifs. Cells with mutations that abolish the interaction between the BRCA1 BRCTs and pSer motifs could be hypersensitive to PARP inhibitor treatment in part because, in the absence of PAR synthesis, the BRCA1/BARD1 complex could neither quickly relocate to nor slowly accumulate at DNA damage sites. This “double hit” might induce tumor cell lethality. This model also provides an explanation for a recent observation that disrupting the interaction

between the BRCA1 BRCTs and phosphoproteins enhances the cytotoxic effect of PARP inhibitors in cancer cells (Langelier et al., 2012).

Notably, PARP inhibitors also kill *BRCA1* null cells for which the aforementioned double-hit model is irrelevant (Drost et al., 2011). It has been shown that impairment of base excision repair by PARP inhibitors aggravates the DNA damage repair deficiency in BRCA1-deficient cells and promotes synthetic lethality (Kummar et al., 2012; Rios and Puhalla, 2011). Moreover, PARP inhibitors can trap PARP1 at DNA damage sites (Murai et al., 2012), blocking normal DNA repair. Together with our data, these observations indicate that there are multiple mechanisms by which PARP inhibition can kill breast cancer cells.

## EXPERIMENTAL PROCEDURES

All other experimental procedures can be found in the [Supplemental Experimental Procedures](#).

### Generation and Purification of PAR

PAR (or biotin-labeled PAR) was synthesized and purified in vitro according to previous work (Fahrer et al., 2007), with some modifications. Briefly, PAR was synthesized in a 15 ml incubation mixture comprising 100 mM Tris-HCl, pH 7.8, 10 mM MgCl<sub>2</sub>, 1 mM NAD<sup>+</sup>, 10 mM dithiothreitol, 60 mg/ml histone H1, 60 mg/ml histone type IIa, 50 mg/ml octameric oligonucleotide GGAATTCC, and 150 nM human PARP1. The reaction was stopped after 60 min by addition of 20 ml ice-cold 20% trichloroacetic acid. Following precipitation, the pellet was washed with ice-cold 99.8% ethanol. Polymer was detached using 0.5 M KOH/50 mM EDTA and was purified by phenol-chloroform extraction and isopropanol precipitation. For the ITC assay, PAR was diluted to the indicated concentrations by the buffer containing 10 mM Na<sub>2</sub>HPO<sub>4</sub> (pH 7.5), 100 mM NaCl.

### GST Fusion Protein Expression and Dot Blot

Glutathione S-transferase (GST) fusion proteins were expressed in *Escherichia coli* or using the Bac-to-Bac Baculovirus expression system (Invitrogen, for CHFR) and purified under standard procedures. Purified GST fusion proteins (10 pmol) were conjugated to the glutathione beads and incubated with PAR (100 pmol, calculated as the ADP-ribose unit) for 2 hr at 4°C. For the competition assays, 30- to 50-mer PAR was fractionated by anion exchange high-performance liquid chromatography (HPLC) protocol as described previously (Fahrer et al., 2007; Kiehlbauch et al., 1993) and used in the experiments. GST-BARD1 BRCTs (10 pmol) were conjugated to the glutathione beads and incubated with PAR (100 pmol, calculated as the ADP-ribose unit) plus 0.1, 1, or 10 nmol ADP-ribose or pSer peptide, respectively, for 2 hr at 4°C. The beads were washed with NETN-100 buffer (0.5% Nonidet P-40, 2 mM EDTA, 50 mM Tris-HCl, pH 8.0, 100 mM NaCl) four times. GST fusion proteins were eluted from beads by glutathione and spotted on to a nitrocellulose membrane. The membrane was blocked with TBST buffer (50 mM Tris-HCl, pH 8.0, 150 mM NaCl, 0.05% Tween 20) supplemented with 5% milk and extensively washed with TBST. After drying in the air, the membrane was examined by anti-PAR antibody.

### Pull-Down Assay

Purified GST fusion proteins (1 pmol) were incubated with biotin-labeled PAR (5 pmol) and streptavidin beads for 2 hr at 4°C. For the competition assays, 30- to 50-mer biotin-PAR was fractionated by anion exchange HPLC protocol and used in the experiments. GST-BARD1 BRCTs (1 pmol) were incubated with biotin-PAR (5 pmol) and streptavidin beads plus 5, 50, or 500 pmol ADP-ribose or pSer peptide, respectively, for 2 hr at 4°C. After washing with NETN-100 buffer four times, the samples were boiled in the SDS sample buffer. The eluates were analyzed by western blot with anti-GST antibody.

### ITC

ITC was carried out at 16°C with an ITC 200 Microcalorimeter (GE Healthcare). Proteins were dialyzed extensively into the buffer containing 10 mM Na<sub>2</sub>HPO<sub>4</sub>,

pH 7.5, 100 mM NaCl at the final concentrations of 20–60 μM. Ligands (PAR, ADP-ribose, or pSer peptide) in the injection syringe were also diluted by the same buffer at the final concentration of 150–750 μM (the concentration of PAR was calculated as the ADP-ribose unit). A typical titration consisted of 19 consecutive 2-μl injections of ligands following a 0.4 μl preinjection of ligands into the protein solution at time intervals of 120 s while stirring at 1,000 rpm. Binding isotherms were integrated and analyzed using the software Origin 7.0 (OriginLab) provided by the manufacturer.

### Laser Microirradiation and Live Cell Imaging

U2OS cells or MEFs transfected with the indicated plasmids were plated on glass-bottomed culture dishes (Mat Tek Corporation). Laser microirradiation was performed using an IX 71 microscope (Olympus) coupled with the MicroPoint Laser Illumination and Ablation System (Photonic Instruments). A 337.1 nm laser diode (3.4 mW) transmits through a specific dye cell and then yields a 365 nm wavelength laser beam that is focused through a 60× UPlanSApo/1.35 oil objective to yield a spot size of 0.5–1 μm. The time of cell exposure to the laser beam was around 3.5 ns. The pulse energy is 170 μJ at 10 Hz. Images were taken by the same microscope with the CellSens software (Olympus). GFP fluorescence at the laser line was converted into a numerical value (relative fluorescence intensity) using Axiovision software (version 4.5). Normalized fluorescent curves from 20 cells from three independent experiments were averaged. The error bars represent the SD.

### Inducible DSB System

U2OS cells stably expressing RFP-I-SceI-GR were used in this system. The synthetic glucocorticoid ligand TA (Sigma) was added (0.1 μM) to induce the translocation of RFP-I-SceI-GR from cytoplasm into nucleus (Zeitlin et al., 2009). Images were taken using the same microscope of laser microirradiation with the CellSens software (Olympus).

### IR Treatment and Colony Formation Assay

Cells were cultured and irradiated 16 hr later with a <sup>137</sup>Cs source at a dose of 10 Gy. After irradiation, cells were lysed at the indicated time points for immunoprecipitation or western blot. For colony formation assay, cells were split into six-well plates and then treated by various doses of IR with or without PJ34. After a 7-day culture, the viable cells were fixed and stained with crystal violet. The number of colonies (more than 50 cells for each colony) was calculated.

## SUPPLEMENTAL INFORMATION

Supplemental Information includes three figures and Supplemental Experimental Procedures and can be found in this article online at <http://dx.doi.org/10.1016/j.ccr.2013.03.025>.

## ACKNOWLEDGMENTS

We thank Dr. Ming Lei for technical support and Drs. Mats Ljungman, Thomas Wilson, Jennifer Keller, and Henry Kuang for editing and proofreading of the manuscript. This work was supported by the National Institutes of Health (CA132755 and CA130899 to X.Y.). X.Y. is a recipient of the Era of Hope Scholar Award from the Department of Defense.

Received: November 21, 2012

Revised: February 15, 2013

Accepted: March 23, 2013

Published: May 13, 2013

## REFERENCES

- Abbott, D.W., Thompson, M.E., Robinson-Benion, C., Tomlinson, G., Jensen, R.A., and Holt, J.T. (1999). BRCA1 expression restores radiation resistance in BRCA1-defective cancer cells through enhancement of transcription-coupled DNA repair. *J. Biol. Chem.* 274, 18808–18812.
- Affar, E.B., Duriez, P.J., Shah, R.G., Sallmann, F.R., Bourassa, S., Küpper, J.H., Bürkle, A., and Poirier, G.G. (1998). Immunodot blot method for the

- detection of poly(ADP-ribose) synthesized in vitro and in vivo. *Anal. Biochem.* 259, 280–283.
- Ali, A.A., Timinszky, G., Arribas-Bosacoma, R., Kozłowski, M., Hassa, P.O., Hassler, M., Ladurner, A.G., Pearl, L.H., and Oliver, A.W. (2012). The zinc-finger domains of PARP1 cooperate to recognize DNA strand breaks. *Nat. Struct. Mol. Biol.* 19, 685–692.
- Au, W.W., and Henderson, B.R. (2005). The BRCA1 RING and BRCT domains cooperate in targeting BRCA1 to ionizing radiation-induced nuclear foci. *J. Biol. Chem.* 280, 6993–7001.
- Birrane, G., Varma, A.K., Soni, A., and Ladas, J.A. (2007). Crystal structure of the BARD1 BRCT domains. *Biochemistry* 46, 7706–7712.
- Botuyan, M.V., Nominé, Y., Yu, X., Juranic, N., Macura, S., Chen, J., and Mer, G. (2004). Structural basis of BACH1 phosphopeptide recognition by BRCA1 tandem BRCT domains. *Structure* 12, 1137–1146.
- Bryant, H.E., Schultz, N., Thomas, H.D., Parker, K.M., Flower, D., Lopez, E., Kyle, S., Meuth, M., Curtin, N.J., and Helleday, T. (2005). Specific killing of BRCA2-deficient tumours with inhibitors of poly(ADP-ribose) polymerase. *Nature* 434, 913–917.
- Bürkle, A. (2001). Physiology and pathophysiology of poly(ADP-ribosylation). *Bioessays* 23, 795–806.
- Celeste, A., Fernandez-Capetillo, O., Kruhlak, M.J., Pilch, D.R., Staudt, D.W., Lee, A., Bonner, R.F., Bonner, W.M., and Nussenzweig, A. (2003). Histone H2AX phosphorylation is dispensable for the initial recognition of DNA breaks. *Nat. Cell Biol.* 5, 675–679.
- Clapperton, J.A., Manke, I.A., Lowery, D.M., Ho, T., Haire, L.F., Yaffe, M.B., and Smerdon, S.J. (2004). Structure and mechanism of BRCA1 BRCT domain recognition of phosphorylated BACH1 with implications for cancer. *Nat. Struct. Mol. Biol.* 11, 512–518.
- D'Amours, D., Desnoyers, S., D'Silva, I., and Poirier, G.G. (1999). Poly(ADP-ribosylation) reactions in the regulation of nuclear functions. *Biochem. J.* 342, 249–268.
- Drost, R., Bouwman, P., Rottenberg, S., Boon, U., Schut, E., Klarenbeek, S., Klijn, C., van der Heijden, I., van der Gulden, H., Wientjens, E., et al. (2011). BRCA1 RING function is essential for tumor suppression but dispensable for therapy resistance. *Cancer Cell* 20, 797–809.
- Dunn, C.A., O'Handley, S.F., Frick, D.N., and Bessman, M.J. (1999). Studies on the ADP-ribose pyrophosphatase subfamily of the nudix hydrolases and tentative identification of trgB, a gene associated with tellurite resistance. *J. Biol. Chem.* 274, 32318–32324.
- Fahrer, J., Kranaster, R., Altmeyer, M., Marx, A., and Bürkle, A. (2007). Quantitative analysis of the binding affinity of poly(ADP-ribose) to specific binding proteins as a function of chain length. *Nucleic Acids Res.* 35, e143.
- Farmer, H., McCabe, N., Lord, C.J., Tutt, A.N., Johnson, D.A., Richardson, T.B., Santarosa, M., Dillon, K.J., Hickson, I., Knights, C., et al. (2005). Targeting the DNA repair defect in BRCA mutant cells as a therapeutic strategy. *Nature* 434, 917–921.
- Fathers, C., Drayton, R.M., Solovieva, S., and Bryant, H.E. (2012). Inhibition of poly(ADP-ribose) glycohydrolase (PARG) specifically kills BRCA2-deficient tumor cells. *Cell Cycle* 11, 990–997.
- Fernández, A., Ribeiro, J.M., Costas, M.J., Pinto, R.M., Canales, J., and Cameselle, J.C. (1996). Specific ADP-ribose pyrophosphatase from *Artemia* cysts and rat liver: effects of nitroprusside, fluoride and ionic strength. *Biochim. Biophys. Acta* 1290, 121–127.
- Fiorillo, C., Nediani, C., Ponziani, V., Giannini, L., Celli, A., Nassi, N., Formigli, L., Perna, A.M., and Nassi, P. (2005). Cardiac volume overload rapidly induces oxidative stress-mediated myocyte apoptosis and hypertrophy. *Biochim. Biophys. Acta* 1741, 173–182.
- Fisher, A.E., Hochegeger, H., Takeda, S., and Caldecott, K.W. (2007). Poly(ADP-ribose) polymerase 1 accelerates single-strand break repair in concert with poly(ADP-ribose) glycohydrolase. *Mol. Cell. Biol.* 27, 5597–5605.
- Fong, P.C., Boss, D.S., Yap, T.A., Tutt, A., Wu, P., Mergui-Roelvink, M., Mortimer, P., Swaisland, H., Lau, A., O'Connor, M.J., et al. (2009). Inhibition of poly(ADP-ribose) polymerase in tumors from BRCA mutation carriers. *N. Engl. J. Med.* 361, 123–134.
- Gasser, A., and Guse, A.H. (2005). Determination of intracellular concentrations of the TRPM2 agonist ADP-ribose by reversed-phase HPLC. *J. Chromatogr. B Analyt. Technol. Biomed. Life Sci.* 821, 181–187.
- Gibson, B.A., and Kraus, W.L. (2012). New insights into the molecular and cellular functions of poly(ADP-ribose) and PARPs. *Nat. Rev. Mol. Cell Biol.* 13, 411–424.
- Harper, J.W., and Elledge, S.J. (2007). The DNA damage response: ten years after. *Mol. Cell* 28, 739–745.
- Hashizume, R., Fukuda, M., Maeda, I., Nishikawa, H., Oyake, D., Yabuki, Y., Ogata, H., and Ohta, T. (2001). The RING heterodimer BRCA1-BARD1 is a ubiquitin ligase inactivated by a breast cancer-derived mutation. *J. Biol. Chem.* 276, 14537–14540.
- Hassa, P.O., Haenni, S.S., Elser, M., and Hottiger, M.O. (2006). Nuclear ADP-ribosylation reactions in mammalian cells: where are we today and where are we going? *Microbiol. Mol. Biol. Rev.* 70, 789–829.
- Hu, Y., Scully, R., Sobhian, B., Xie, A., Shestakova, E., and Livingston, D.M. (2011). RAP80-directed tuning of BRCA1 homologous recombination function at ionizing radiation-induced nuclear foci. *Genes Dev.* 25, 685–700.
- Huen, M.S., Sy, S.M., and Chen, J. (2010). BRCA1 and its toolbox for the maintenance of genome integrity. *Nat. Rev. Mol. Cell Biol.* 11, 138–148.
- Huen, M.S., Grant, R., Manke, I., Minn, K., Yu, X., Yaffe, M.B., and Chen, J. (2007). RNF8 transduces the DNA-damage signal via histone ubiquitylation and checkpoint protein assembly. *Cell* 131, 901–914.
- Ishitobi, M., Miyoshi, Y., Hasegawa, S., Egawa, C., Tamaki, Y., Monden, M., and Noguchi, S. (2003). Mutational analysis of BARD1 in familial breast cancer patients in Japan. *Cancer Lett.* 200, 1–7.
- Karras, G.I., Kustatscher, G., Buhecha, H.R., Allen, M.D., Pugieux, C., Sait, F., Bycroft, M., and Ladurner, A.G. (2005). The macro domain is an ADP-ribose binding module. *EMBO J.* 24, 1911–1920.
- Kiehbauch, C.C., Aboul-El, N., Jacobson, E.L., Ringer, D.P., and Jacobson, M.K. (1993). High resolution fractionation and characterization of ADP-ribose polymers. *Anal. Biochem.* 208, 26–34.
- Kim, M.Y., Zhang, T., and Kraus, W.L. (2005). Poly(ADP-ribosylation) by PARP-1: 'PAR-laying' NAD<sup>+</sup> into a nuclear signal. *Genes Dev.* 19, 1951–1967.
- Kim, H., Chen, J., and Yu, X. (2007). Ubiquitin-binding protein RAP80 mediates BRCA1-dependent DNA damage response. *Science* 316, 1202–1205.
- King, M.C., Marks, J.H., and Mandell, J.B.; New York Breast Cancer Study Group. (2003). Breast and ovarian cancer risks due to inherited mutations in BRCA1 and BRCA2. *Science* 302, 643–646.
- Kolas, N.K., Chapman, J.R., Nakada, S., Ylanko, J., Chahwan, R., Sweeney, F.D., Panier, S., Mendez, M., Wildenhain, J., Thomson, T.M., et al. (2007). Orchestration of the DNA-damage response by the RNF8 ubiquitin ligase. *Science* 318, 1637–1640.
- Koonin, E.V., Altschul, S.F., and Bork, P. (1996). BRCA1 protein products... Functional motifs... *Nat. Genet.* 13, 266–268.
- Kummar, S., Chen, A., Parchment, R.E., Kinders, R.J., Ji, J., Tomaszewski, J.E., and Doroshow, J.H. (2012). Advances in using PARP inhibitors to treat cancer. *BMC Med.* 10, 25.
- Langelier, M.F., Planck, J.L., Roy, S., and Pascal, J.M. (2012). Structural basis for DNA damage-dependent poly(ADP-ribosylation) by human PARP-1. *Science* 336, 728–732.
- Mailand, N., Bekker-Jensen, S., Fastrup, H., Melander, F., Bartek, J., Lukas, C., and Lukas, J. (2007). RNF8 ubiquitylates histones at DNA double-strand breaks and promotes assembly of repair proteins. *Cell* 131, 887–900.
- Manke, I.A., Lowery, D.M., Nguyen, A., and Yaffe, M.B. (2003). BRCT repeats as phosphopeptide-binding modules involved in protein targeting. *Science* 302, 636–639.
- Masson, M., Niedergang, C., Schreiber, V., Muller, S., Menissier-de Murcia, J., and de Murcia, G. (1998). XRCC1 is specifically associated with poly(ADP-ribose) polymerase and negatively regulates its activity following DNA damage. *Mol. Cell. Biol.* 18, 3563–3571.

- Meza, J.E., Brzovic, P.S., King, M.C., and Klevit, R.E. (1999). Mapping the functional domains of BRCA1. Interaction of the ring finger domains of BRCA1 and BARD1. *J. Biol. Chem.* 274, 5659–5665.
- Miki, Y., Swensen, J., Shattuck-Eidens, D., Futreal, P.A., Harshman, K., Tavtigian, S., Liu, Q., Cochran, C., Bennett, L.M., Ding, W., et al. (1994). A strong candidate for the breast and ovarian cancer susceptibility gene BRCA1. *Science* 266, 66–71.
- Miró, A., Costas, M.J., García-Díaz, M., Hernández, M.T., and Cameselle, J.C. (1989). A specific, low Km ADP-ribose pyrophosphatase from rat liver. *FEBS Lett.* 244, 123–126.
- Morris, J.R., Keep, N.H., and Solomon, E. (2002). Identification of residues required for the interaction of BARD1 with BRCA1. *J. Biol. Chem.* 277, 9382–9386.
- Murai, J., Huang, S.Y., Das, B.B., Renaud, A., Zhang, Y., Doroshow, J.H., Ji, J., Takeda, S., and Pommier, Y. (2012). Trapping of PARP1 and PARP2 by Clinical PARP Inhibitors. *Cancer Res.* 72, 5588–5599.
- Okano, S., Lan, L., Caldecott, K.W., Mori, T., and Yasui, A. (2003). Spatial and temporal cellular responses to single-strand breaks in human cells. *Mol. Cell Biol.* 23, 3974–3981.
- Rahman, N., and Stratton, M.R. (1998). The genetics of breast cancer susceptibility. *Annu. Rev. Genet.* 32, 95–121.
- Ribeiro, J.M., Cameselle, J.C., Fernández, A., Canales, J., Pinto, R.M., and Costas, M.J. (1995). Inhibition and ADP-ribose pyrophosphatase-I by nitric-oxide-generating systems: a mechanism linking nitric oxide to processes dependent on free ADP-ribose. *Biochem. Biophys. Res. Commun.* 213, 1075–1081.
- Ribeiro, J.M., Carloto, A., Costas, M.J., and Cameselle, J.C. (2001). Human placenta hydrolases active on free ADP-ribose: an ADP-sugar pyrophosphatase and a specific ADP-ribose pyrophosphatase. *Biochim. Biophys. Acta* 1526, 86–94.
- Rios, J., and Puhalla, S. (2011). PARP inhibitors in breast cancer: BRCA and beyond. *Oncology (Huntingt.)* 25, 1014–1025.
- Rodriguez, M., Yu, X., Chen, J., and Songyang, Z. (2003). Phosphopeptide binding specificities of BRCA1 COOH-terminal (BRCT) domains. *J. Biol. Chem.* 278, 52914–52918.
- Rouleau, M., Patel, A., Hendzel, M.J., Kaufmann, S.H., and Poirier, G.G. (2010). PARP inhibition: PARP1 and beyond. *Nat. Rev. Cancer* 10, 293–301.
- Roy, R., Chun, J., and Powell, S.N. (2011). BRCA1 and BRCA2: different roles in a common pathway of genome protection. *Nat. Rev. Cancer* 12, 68–78.
- Ruscetti, T., Lehnert, B.E., Halbrook, J., Le Trong, H., Hoekstra, M.F., Chen, D.J., and Peterson, S.R. (1998). Stimulation of the DNA-dependent protein kinase by poly(ADP-ribose) polymerase. *J. Biol. Chem.* 273, 14461–14467.
- Sauer, M.K., and Andrulis, I.L. (2005). Identification and characterization of missense alterations in the BRCA1 associated RING domain (BARD1) gene in breast and ovarian cancer. *J. Med. Genet.* 42, 633–638.
- Schreiber, V., Dantzer, F., Ame, J.C., and de Murcia, G. (2006). Poly(ADP-ribose): novel functions for an old molecule. *Nat. Rev. Mol. Cell Biol.* 7, 517–528.
- Scully, R., and Livingston, D.M. (2000). In search of the tumour-suppressor functions of BRCA1 and BRCA2. *Nature* 408, 429–432.
- Scully, R., Chen, J., Ochs, R.L., Keegan, K., Hoekstra, M., Feunteun, J., and Livingston, D.M. (1997). Dynamic changes of BRCA1 subnuclear location and phosphorylation state are initiated by DNA damage. *Cell* 90, 425–435.
- Shen, S.X., Weaver, Z., Xu, X., Li, C., Weinstein, M., Chen, L., Guan, X.Y., Ried, T., and Deng, C.X. (1998). A targeted disruption of the murine Brca1 gene causes gamma-irradiation hypersensitivity and genetic instability. *Oncogene* 17, 3115–3124.
- Sobhian, B., Shao, G., Lilli, D.R., Culhane, A.C., Moreau, L.A., Xia, B., Livingston, D.M., and Greenberg, R.A. (2007). RAP80 targets BRCA1 to specific ubiquitin structures at DNA damage sites. *Science* 316, 1198–1202.
- Soutoglou, E., Dorn, J.F., Sengupta, K., Jasin, M., Nussenzweig, A., Ried, T., Danuser, G., and Misteli, T. (2007). Positional stability of single double-strand breaks in mammalian cells. *Nat. Cell Biol.* 9, 675–682.
- Thai, T.H., Du, F., Tsan, J.T., Jin, Y., Phung, A., Spillman, M.A., Massa, H.F., Muller, C.Y., Ashfaq, R., Mathis, J.M., et al. (1998). Mutations in the BRCA1-associated RING domain (BARD1) gene in primary breast, ovarian and uterine cancers. *Hum. Mol. Genet.* 7, 195–202.
- Turner, N., Tutt, A., and Ashworth, A. (2004). Hallmarks of ‘BRCAness’ in sporadic cancers. *Nat. Rev. Cancer* 4, 814–819.
- Venkiteswaran, A.R. (2002). Cancer susceptibility and the functions of BRCA1 and BRCA2. *Cell* 108, 171–182.
- Vilchez Larrea, S.C., Alonso, G.D., Schlesinger, M., Torres, H.N., Flawiá, M.M., and Fernández Villamil, S.H. (2011). Poly(ADP-ribose) polymerase plays a differential role in DNA damage-response and cell death pathways in *Trypanosoma cruzi*. *Int. J. Parasitol.* 41, 405–416.
- Wang, B., Matsuoka, S., Ballif, B.A., Zhang, D., Smogorzewska, A., Gygi, S.P., and Elledge, S.J. (2007). Abraxas and RAP80 form a BRCA1 protein complex required for the DNA damage response. *Science* 316, 1194–1198.
- Williams, R.S., Lee, M.S., Hau, D.D., and Glover, J.N. (2004). Structural basis of phosphopeptide recognition by the BRCT domain of BRCA1. *Nat. Struct. Mol. Biol.* 11, 519–525.
- Wu, L.C., Wang, Z.W., Tsan, J.T., Spillman, M.A., Phung, A., Xu, X.L., Yang, M.C., Hwang, L.Y., Bowcock, A.M., and Baer, R. (1996). Identification of a RING protein that can interact in vivo with the BRCA1 gene product. *Nat. Genet.* 14, 430–440.
- Ying, W., Seigny, M.B., Chen, Y., and Swanson, R.A. (2001). Poly(ADP-ribose) glycohydrolase mediates oxidative and excitotoxic neuronal death. *Proc. Natl. Acad. Sci. USA* 98, 12227–12232.
- Yu, X., Chini, C.C., He, M., Mer, G., and Chen, J. (2003). The BRCT domain is a phospho-protein binding domain. *Science* 302, 639–642.
- Zeitlin, S.G., Baker, N.M., Chapados, B.R., Soutoglou, E., Wang, J.Y., Berns, M.W., and Cleveland, D.W. (2009). Double-strand DNA breaks recruit the centromeric histone CENP-A. *Proc. Natl. Acad. Sci. USA* 106, 15762–15767.